Contents

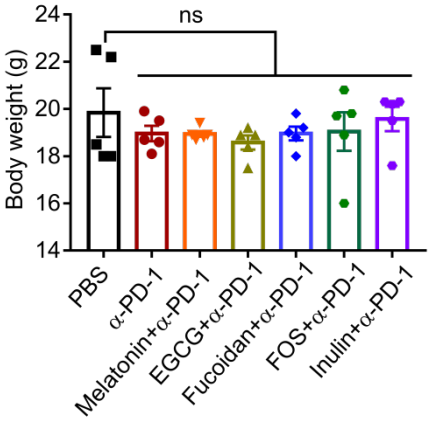

Supplementary Fig. S1. Mouse bodyweight changes after combination treatments. Mice were treated as in Fig.2a, and the animals were weighed on day 20. Data represent mean ± SEM (*n* = 5 biologically independent samples), ns, not significant, analyzed by one-way ANOVA with Bonferroni's multiple comparisons test.

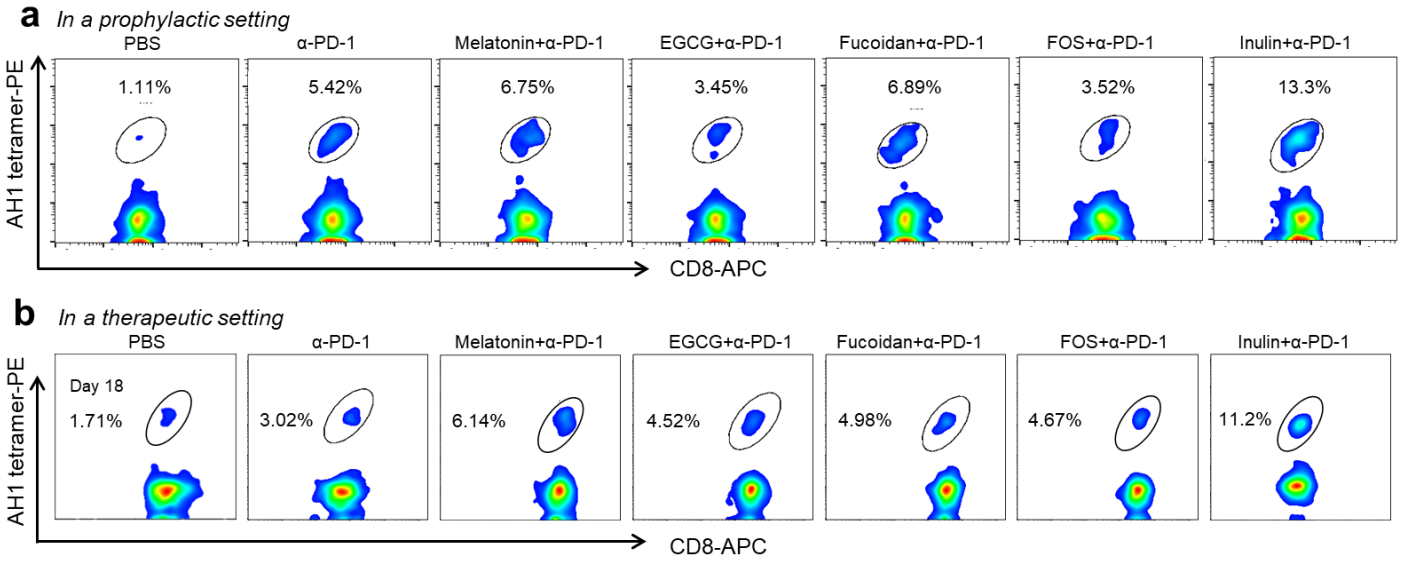

Supplementary Fig. S2. The representative scatter plots of AH1-specific CD8$^+$ T cells in peripheral blood. a, CT26 tumor-bearing mice were treated as in Fig. 2a. Shown are the representative scatter plots of AH1-specific CD8$^+$ T cells in peripheral blood on day 22. **b**, CT26 tumor-bearing mice were treated as in Fig. 2f. Shown are the representative scatter plots of AH1-specific CD8$^+$ T cells on day 18, analyzed by flow cytometry.

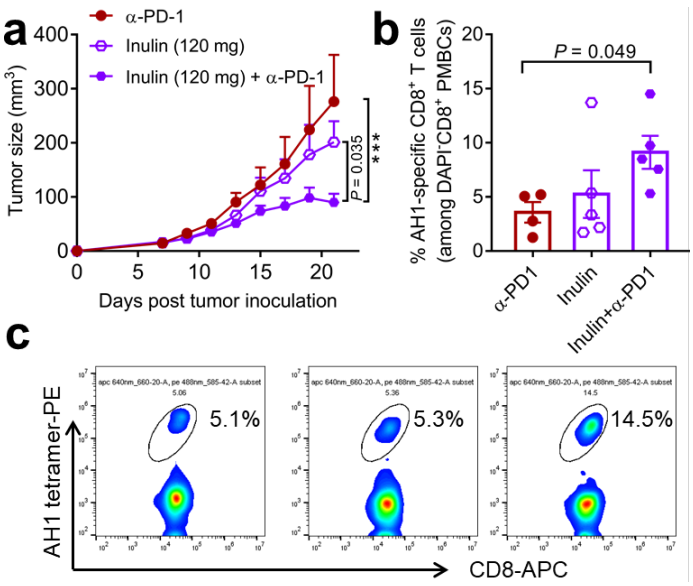

Supplementary Fig. S3. Inulin synergizes with α-PD-1 therapy. CT26 tumor-bearing mice were treated as in Fig. 2f. Shown are the (**a**) average tumor growth curves, (**b**) frequencies of AH1-specific $CD8^+$ T cells, and (**c**) representative scatter plots in peripheral blood on day 17 analyzed by flow cytometry. Data represent mean ± SEM (n = 4-5 biologically independent samples), ***P < 0.001, analyzed by two-way ANOVA (**a**), or one-way ANOVA (**b**) with Bonferroni's multiple comparisons test.

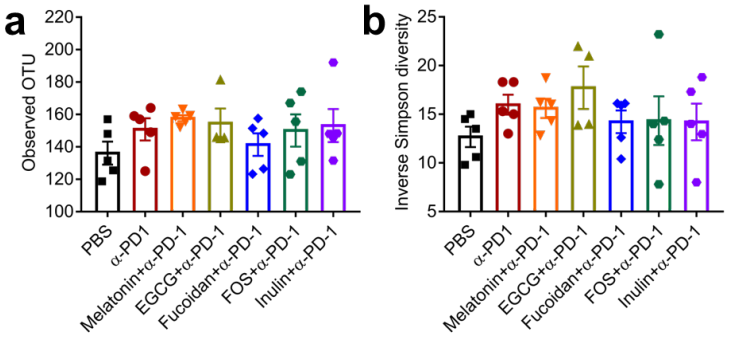

Supplementary Fig. S4. Analysis of the gut microbiota. CT26 tumor-bearing mice were treated as in Fig. 2f. Fecal pellets were collected on day 21. Shown are the (**a**) OTU number, (**b**) inverse Simpson diversity. Data represent mean ± SEM (n = 5 biologically independent samples).

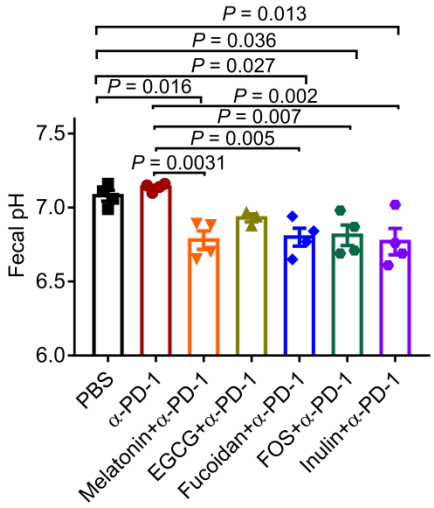

Supplementary Fig. S5. Fecal pH analysis. CT26 tumor-bearing mice were treated as in Fig. 2f. Shown are the fecal pHs on day 20. Data represent mean ± SEM (*n* = 4 biologically independent samples), analyzed by one-way ANOVA with Bonferroni's multiple comparisons test.

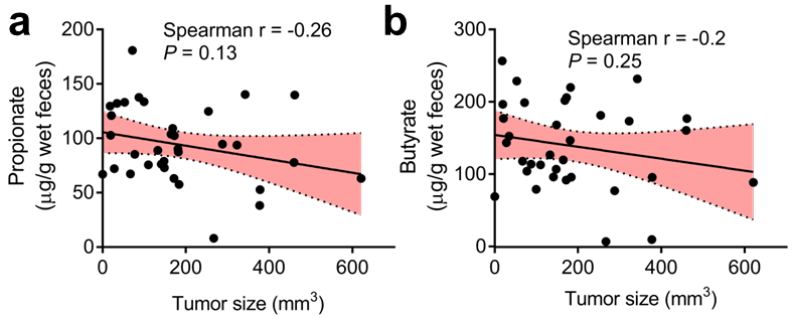

Supplementary Fig. S6. Spearman's correlation analysis. CT26 tumor-bearing mice were treated as in Fig. 2f. Shown are the Spearman's correlations between the tumor sizes and the concentrations of (**a**) propionate and (**b**) butyrate. Shaded band indicates 95% CI of the values fitted by linear regression.

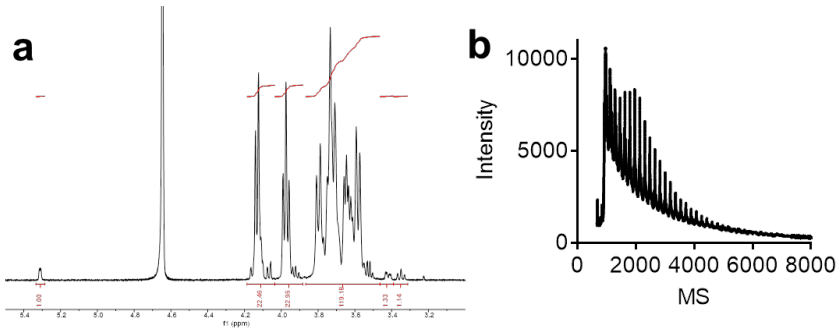

Supplementary Fig. S7. Characterizations of inulin. Shown are the (**a**) ^{1}H NMR spectrum and (**b**) matrix-assisted laser desorption ionization time-of-flight (MALDI-TOF) mass spectrum of inulin employed for inulin gel formation.

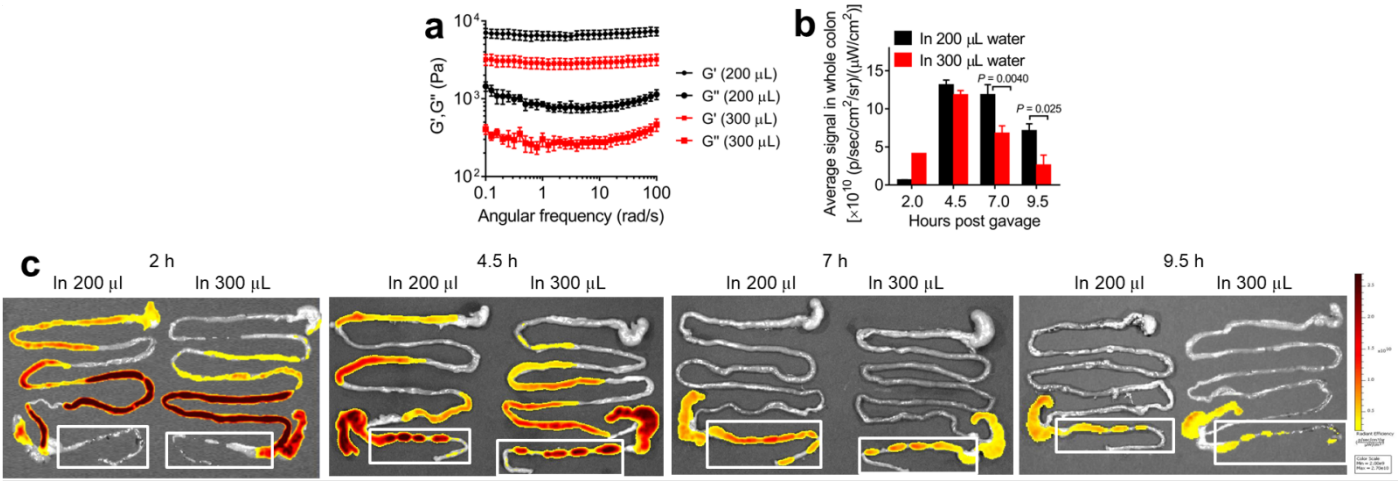

Supplementary Fig. S8. Colon retention of inulin gel with different gel strength. 60 mg of Inulin gel was prepared in 200 or 300 µL DI water. Shown are (**a**) G' (elastic modulus), G'' (viscous modulus) of inulin gel. Mice were orally gavaged with FITC-labeled inulin gel (60 mg/dose) in 200 or 300 µL DI water, followed by visualization of the gastrointestinal tract. Shown are the (**b**) signal in whole colon, and (**c**) the representative fluorescence imaging at different time points. Data represent mean ± SEM (*n* = 4 (**a**), *n* = 3 (**b**) biologically independent samples). Data were analyzed by two-way ANOVA with Bonferroni's multiple comparisons test.

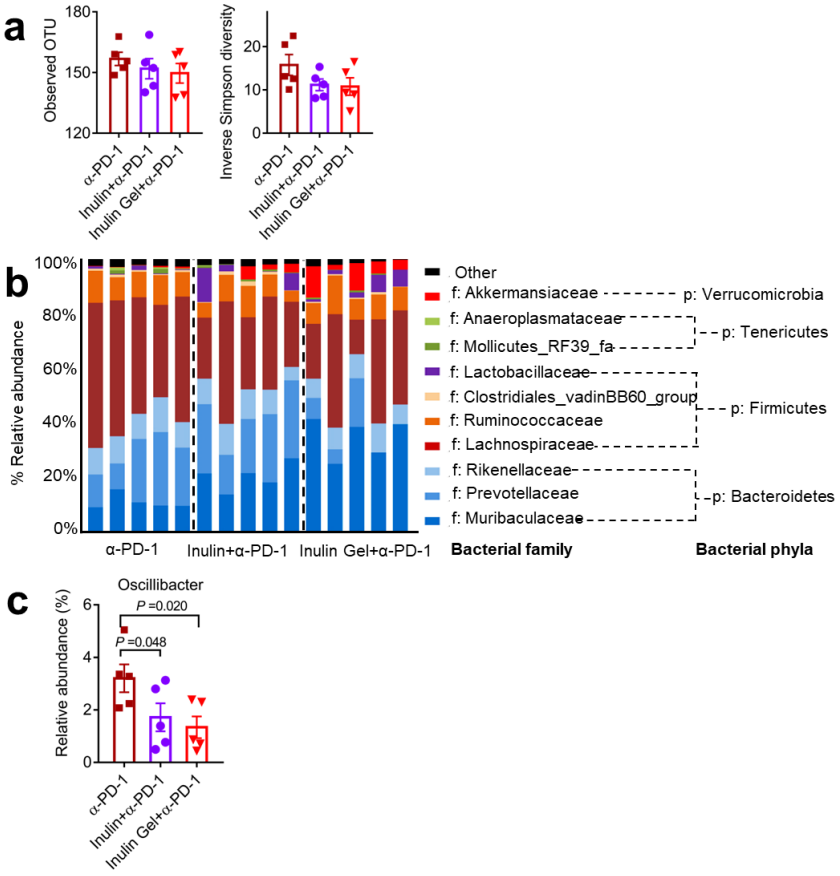

Supplementary Fig. S9. Gut microbiota analysis. CT26 tumor-bearing BALB/c mice were treated as in Fig. 4g. Shown are (**a**) OTU number, inverse Simpson diversity, (**b**) microbial community analysis in phylum and family levels, p: phylum level, f: family level, (**c**) relative abundances of *Oscillibacter* in the genus level on day 21. Data represent mean ± SEM (*n* = 5 biologically independent samples), analyzed by one-way ANOVA with Bonferroni's multiple comparisons test.

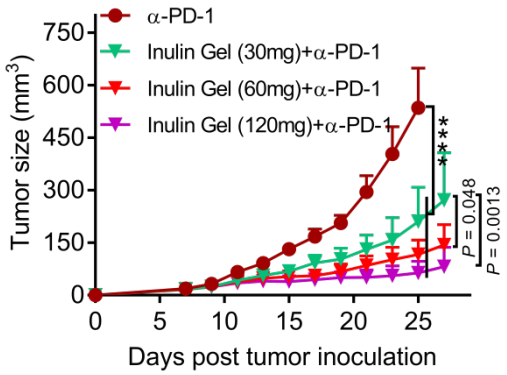

Supplementary Fig. S10. The synergy effect between inulin gel and α-PD-1 is gel dose dependent. CT26 tumor-bearing mice were treated as in Fig. 5a. Shown are the average tumor growth curves for groups treated with varying doses of inulin gel. Data represent mean ± SEM (*n* = 5 biologically independent samples), ****$P < 0.0001$, analyzed by two-way ANOVA with Bonferroni's multiple comparisons test.

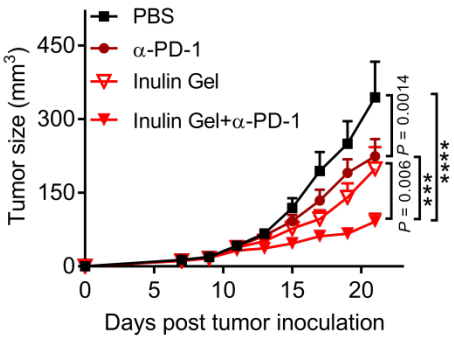

Supplementary Fig. S11. Inulin gel synergizes with α-PD-1 therapy. CT26 tumor-bearing mice were treated as in Fig. 5a. Shown are the average tumor growth curves. Data represent mean ± SEM (*n* = 10 biologically independent samples), ***$P < 0.001$, ****$P < 0.0001$, analyzed by two-way ANOVA with Bonferroni's multiple comparisons test.

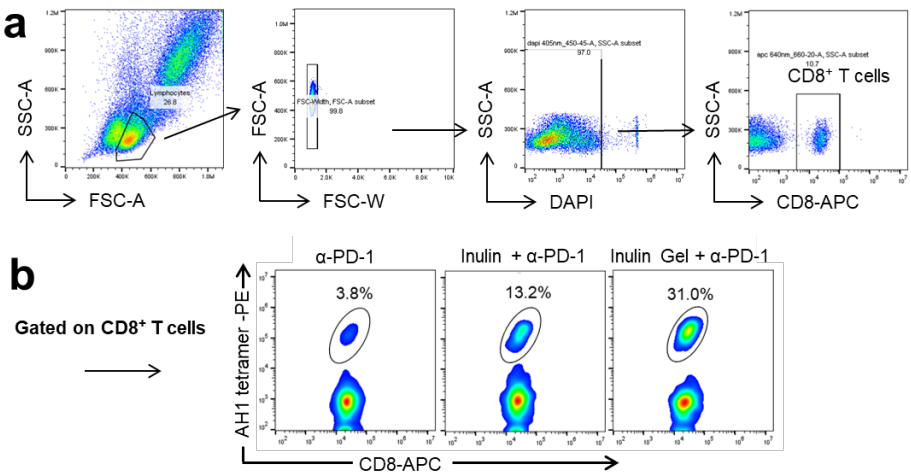

Supplementary Fig. S12. AH1-specific CD8$^+$ T cells analysis in PBMCs. CT26 tumor-bearing mice were treated as in Fig. 5a. Shown are the (**a**) gating strategy for analyzing AH1-specific CD8$^+$ T cells and (**b**) representative scatter plots of AH1-specific CD8$^+$ T cells in peripheral blood on day 21.

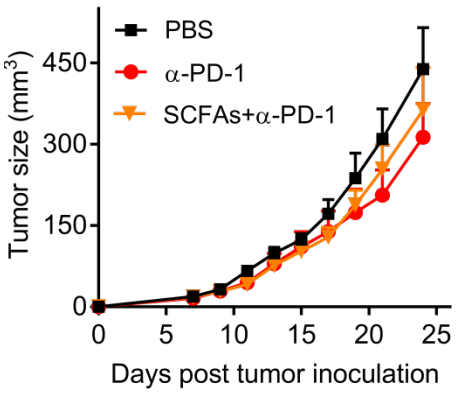

Supplementary Fig. S13. SCFAs in drinking water can not improve α-PD-1 efficacy. CT26 tumor-bearing mice were maintained on drinking water containing 120 mM sodium chloride, or the mixture of SCFAs (65 mM sodium acetate, 25 mM sodium propionate, and 30 mM sodium butyrate). α-PD-1 administration was performed on days 11, 14, 17, and 20 (100 μg/dose). Shown are the average tumor growth curves. Data represent mean ± SEM (*n* = 5 biologically independent samples).

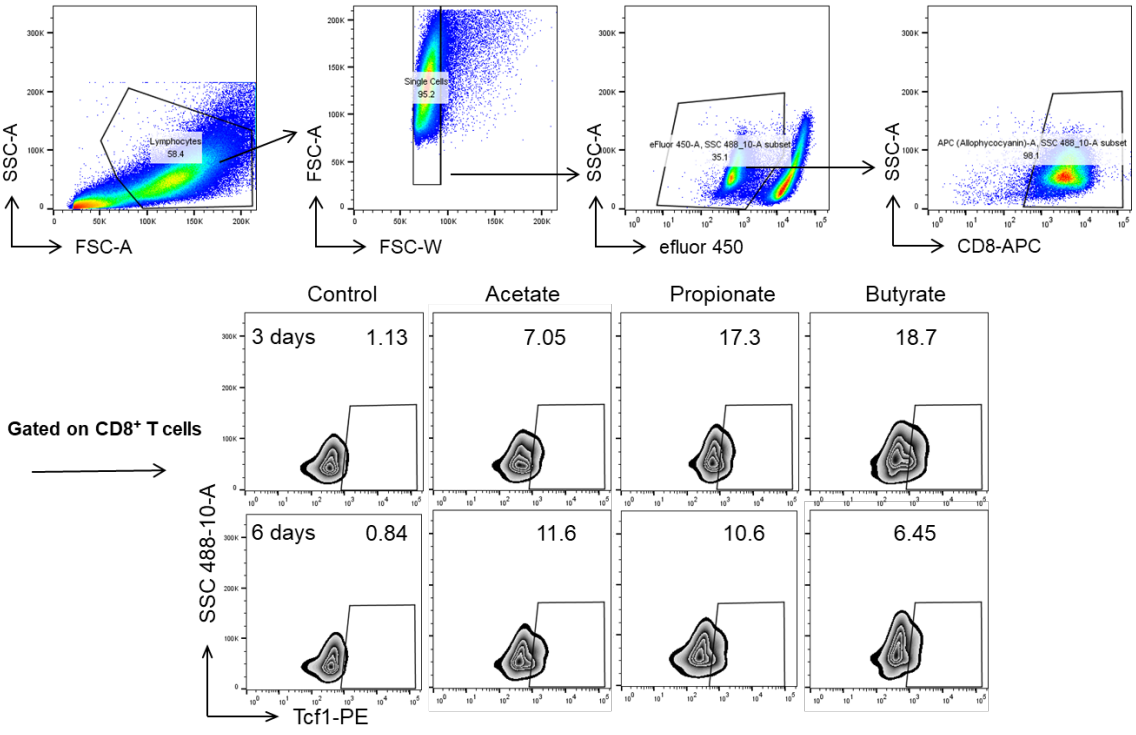

Supplementary Fig. S14. SCFAs modulate Tcf1 expressions on CD8$^+$ T cells. OVA-specific OT-I T cells were treated as in Fig. 7a. Shown are the gating strategy and representative scatter plots of Tcf1$^+$CD8$^+$ T cells after 3 days or 6 days incubation with 400 μM SCFAs.

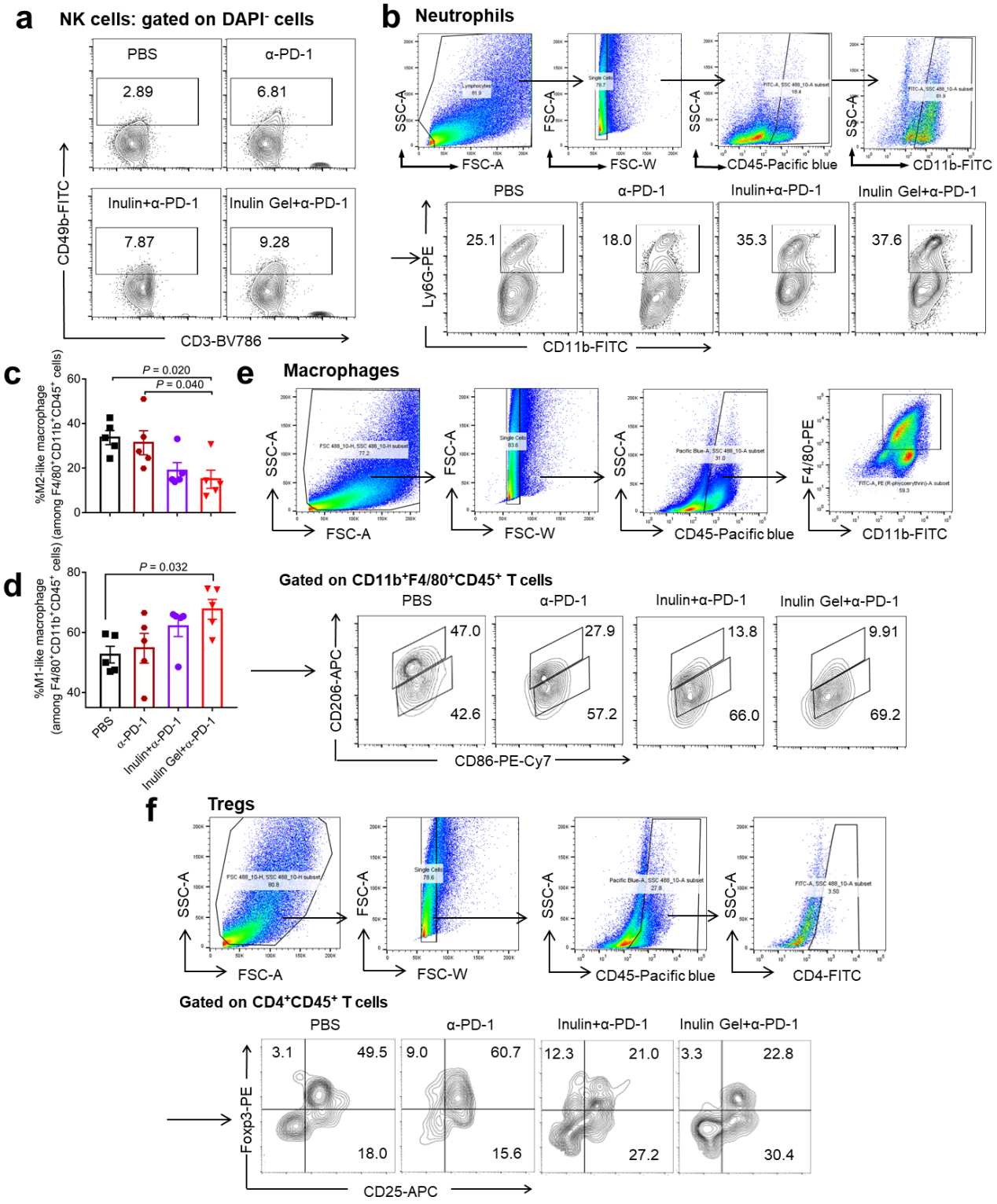

Supplementary Fig. S15. Intratumoral microenvironment analysis. CT26 tumor-bearing BALB/c mice were treated as in Fig. 5a. Shown are the (**a**) representative scatter plots of NK cells; (**b**) the gating strategy for $Ly6G^+CD11b^+$ neutrophils and representative scatter plots; frequencies of (**c**) M2-like macrophages, (**d**) M1-like macrophages, and (**e**) gating strategy for analyzing $CD11b^+F4/80^+CD45^+$ macrophage cells as well as their representative scatter plots; and (**f**) the gating strategy for $CD4^+CD25^+Foxp3^+$ Tregs and representative scatter plots in tumor on day 21. Data represent mean ± SEM (n = 5 biologically independent samples), analyzed by one-way ANOVA with Bonferroni's multiple comparisons test.

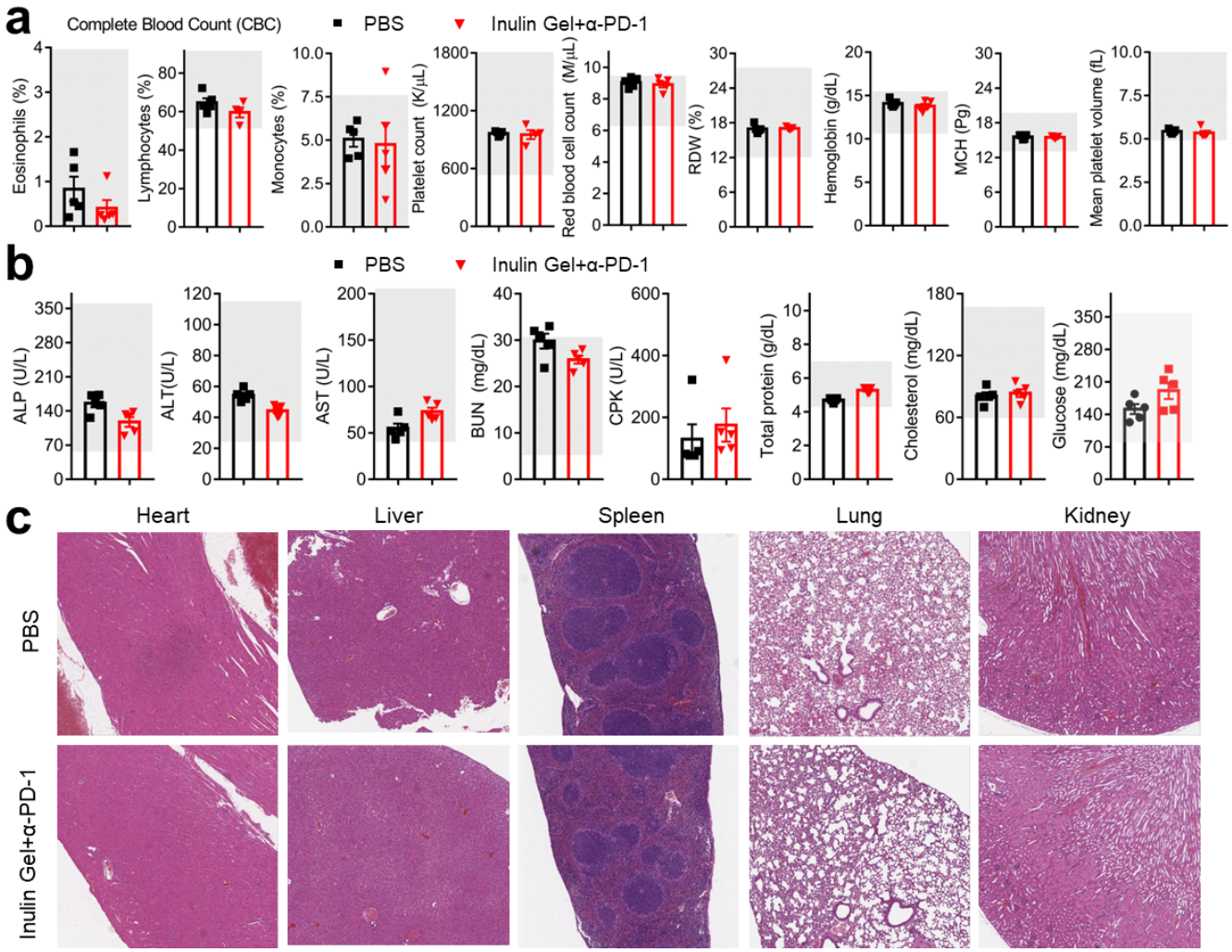

Supplementary Fig. S16. Safety evalution of inulin gel plus α-PD-1 treatment. CT26 tumor-bearing BALB/c mice were treated as in Fig. 5a. Shown are (**a**) the complete blood count panel, including eosinophils, lymphocytes, monocytes, platelet count, red blood cell count, RDW, hemoglobin, MCH, and mean platelet volume; (**b**) the biochemistry panel, including ALP, ALT, AST, BUN, CPK, total protein, cholesterol and glucose; (**c**) H&E staining of heart, liver, spleen, lung, kidneys after inulin gel plus α-PD-1 treatment on day 29. The gray area in (**a**) and (**b**) indicates the normal range of complete blood count and biochemistry in mice. Data represent mean ± SEM (*n* = 5 biologically independent samples).